

Development of Spacecraft Radiated Susceptibility RS103 Requirements From Modeling Methods

Pablo S. Narvaez, *Senior Member, IEEE*, Nacer E. Chahat, *Senior Member, IEEE*, and Edward C. Gonzales
Jet Propulsion Laboratory, California Institute of Technology
Pasadena, California 91109

Email: pablo.narvaez@jpl.nasa.gov, nacer.e.chahat@jpl.nasa.gov, edward.c.gonzales@jpl.nasa.gov

Abstract— In defining radiated susceptibility requirements for a spacecraft with multiple number of receivers and transmitters in close proximity to each other, the main objective of an RF coupling analysis is to determine if the mechanical configuration of the receiver and transmitter antennas presents a risk to the functionality and safety of sensitive science instruments on the payload as a result of unintended RF coupling. Where there is a potential risk for interference or permanent damage, further analysis is required to evaluate the feasibility of mitigation schemes, such as mechanical reconfiguration of antennas or additional RF filtering. From these coupling analysis results, radiated susceptibility RS103 requirements are derived to better reflect actual requirement levels with adequate test margins.

Keywords—radiated susceptibility, RF coupling, electromagnetic compatibility, EMC requirements, near field, electromagnetic interference, RF filtering, coupling path.

I. INTRODUCTION

Typical general MIL-STD 461 requirements cannot be used for applying radiated susceptibility (RS) requirements where spacecraft high powered transmitters and sensitive receivers are co-located in close proximity to each other. An initial first-order analysis of the radio frequency (RF) coupling between the various transmitters and receivers is highly recommended to ensure proper RS103 requirements are applied. It does not make sense to simply apply radiated susceptibility requirements on a flight system if the RS requirement levels are harmful to sensitive receivers to the point of causing permanent damage. Moreover, before any radiated susceptibility requirements are levied, it is highly recommended that an initial detailed RF coupling assessment be performed to ensure system compatibility amongst all receivers and transmitters so that no interference results from being co-located so close to each other.

From the results of the initial RF coupling analysis between identified victims (receivers) and sources (transmitters), an iterative process is initiated resulting in mechanical layout configuration changes or transmitter and receiver filtering schemes. An example of this approach is presented in this paper as applied on the Surface Water and Ocean Topography (SWOT) spacecraft (Figure 1). The SWOT mission with its wide-swath altimetry technology is a means of completely covering the world's oceans and freshwater bodies with

repeated high-resolution elevation measurements. SWOT is truly a multi-disciplinary cooperative international effort.

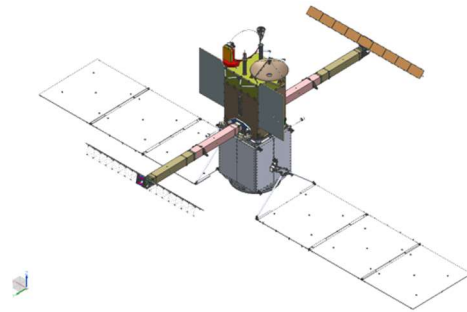


Fig. 1. Surface Water and Ocean Topography Spacecraft

On the SWOT spacecraft, there are multiple number of sensitive RF receivers and high-powered transmitters in closed proximity to each other. These instruments are mounted on the nadir deck (Figure 2 a, b) of the spacecraft, which includes a high powered X-Band transmitter, an Advanced Microwave Radiometer (AMR), Nadir Altimeter (NA), Doppler Orbitography and Radiopositioning Integrated by Satellite (DORIS), and Ka-band Radar Interferometer (KaRIn).

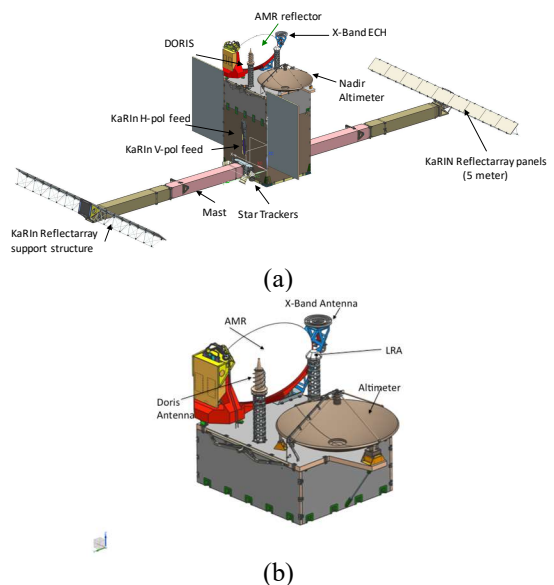


Fig. 2. (a) SWOT Payload, and (b) Nadir Deck Science Instrument Locations

AMR is an example of the sensitivity of the receivers on SWOT. AMR is comprised of a set of radiometric receivers, with center frequencies and noise bandwidths listed in Table I.

TABLE I. AMR RECEIVER CENTER FREQUENCIES AND NOISE BANDWIDTHS

| Channel | Center Frequency | Noise Bandwidth |
|---------|------------------|-----------------|
| # | GHz | MHz |
| 1 | 18.7 | 200 |
| 2 | 23.8 | 400 |
| 3 | 34.0 | 700 |

Each AMR radiometric channel is sensitive to radio frequency interference (RFI) within and adjacent to its noise bandwidth. The radiometric data can be corrupted by direct radiation coupled into the receiver's noise bandwidth and indirect, from radiation coupled into the bandwidth of the receiver's first two stages of amplification, causing low-level gain compression.

To this end, an RF coupling analysis between transmitters and receivers was performed on all these instruments in order to mitigate the risk that payload transmitters such as the X-band transmitter and KaRIn radar presented to the functionality of the other sensitive receivers as a result of their physical location on the nadir deck. A matrix of victims and sources was therefore prioritized as shown in Table II.

TABLE II. SWOT VICTIMS AND SOURCES MATRIX

| Receiver Victims | Transmitter Sources | | |
|------------------|--|---|--|
| | X-Band | KaRIn | Nadir Altimeter |
| KaRIn | X-Band interfering with Ka-Band | Not Applicable | C and Ku-Bands interfering with Ka-Band |
| Nadir Altimeter | X-Band interfering with C and Ku-Bands | Ka-Band interfering with C and Ku-Bands | Not Applicable |
| DORIS | X-Band interfering with UHF and S-Band | Ka-Band interfering with UHF and S-Band | C and Ku-Bands interfering with UHF and S-Band |
| AMR | X-Band interfering with channels 1-3 | Ka-Band interfering with channels 1-3 | C and Ku-Bands interfering with channels 1-3 |

II. INITIAL FIRST ORDER COUPLING ANALYSIS

All coupling pairs were analyzed to a first-order. Where the capability existed, a more detailed analysis was performed using computer-aided tools, which included ANSYS HFSS for near-field modeling and GRASP for far-field modeling (physical optics regime). In general, the RF coupling analysis involved source-victim pairs located in the physical optics regime, so GRASP was favored in most cases. Detailed modeling of the X-band and KaRIn transmitters were performed as a transmitter source to its receiver victims.

Where possible, worst-case assumptions were made to ensure margin. A first-order analysis was conducted for all source-victim pairs slated for analysis using the Friis transmission equation.

A. Friis transmission formula

The coupling between two antennas can be assessed as originally described by Friis shown in equation (1):

$$c = P_r / P_t = G_t(\theta_t, \varphi_t) \cdot G_r(\theta_r, \varphi_r) \frac{\lambda^2}{(4\pi r)^2} \quad (1)$$

where P_r is the received power, P_t is the transmitted power, G_r is the receiver antenna gain, and G_t is the transmitting antenna gain.

The coupling can also be expressed in equation (2):

$$c = \frac{b_r}{a_t} = -j \frac{1}{2} \frac{e^{-jkr}}{kr} \bar{E}_{t, \text{far}}(\theta_t, \varphi_t) \cdot \bar{E}_{r, \text{far}}(\theta_r, \varphi_r) \quad (2)$$

where $E_{t, \text{far}}$ and $E_{r, \text{far}}$ are the far field radiated by the transmitting and receiving antenna, respectively, r is the distance between the two antennas, b_r is the received signal, a_t is the transmitted signal, and k is the wavenumber.

The Friis equation requires that the two antennas are in the far field of each other. It is commonly accepted that the far field of an antenna exists for distances greater than the Fraunhofer region distance R given by equation (3):

$$R = \frac{2D^2}{\lambda} \quad (3)$$

where D is the diameter of the antenna as seen from the field point.

Implicit in the use of this equation is that transmit-receive pairs are in the far field. This assumption is generally good except for cases where wavelength is significantly smaller than the radiating aperture and the transmit-receive pair are in close proximity. This does occur on SWOT (for example, DORIS and Nadir Altimeter) and first-order results had significant error bars. In many cases, the first-order analysis yielded results within 10 dB of the GRASP value and tended to be more conservative.

B. Coupling to an antenna in the near field

The coupling between two antennas can be assessed even if one or both of the antennas are in the near field of the other using, as implemented in TICRA GRASP, the following equation (4):

$$c = \frac{b_r}{a_t} = -j \frac{1}{2} k r e^{jkr} \bar{E}_{t, \text{far}}(r, \theta_t, \varphi_t) \cdot \bar{E}_{r, \text{far}}(r, \theta_r, \varphi_r) \quad (4)$$

In this case, a correct near-field can be calculated using a spherical wave expansion (SWE). It is therefore important to make sure that each antenna is outside of each other SWE sphere (the SWE is valid outside the sphere). This approach is applied to assess the coupling between feeds.

III. COUPLING ASSESSMENT BETWEEN THE KARIN AND X-BAND TELECOM

The KaRIn instrument contains two Ka-band Synthetic Aperture RADAR antennas at opposite ends of a 10-meter boom with both antennas transmitting and receiving the emitted radar pulses along both sides of the orbital track (see Figure 3).

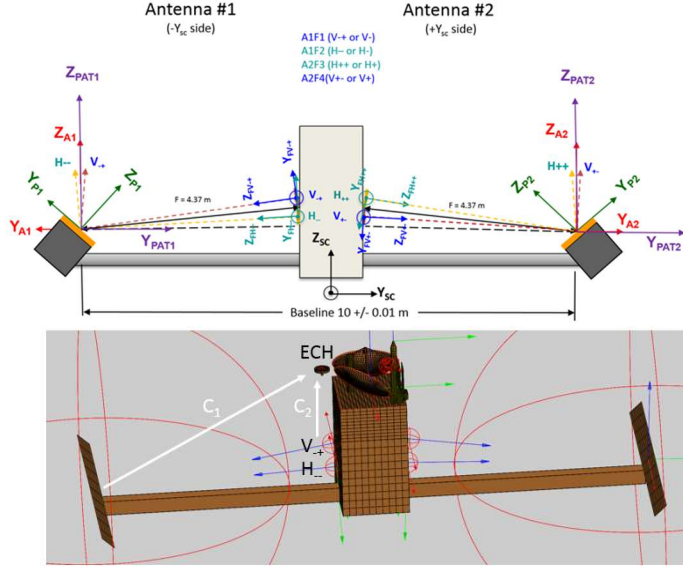


Fig. 3. (Top) Reflectarray configuration. (b) (Bottom) Tica GRASP model of SWOT spacecraft used for coupling assessment between KaRIn and X-band telecom. The spherical expansion sphere of the reflectarray and feeds are illustrated in red. C_1 is the coupling between the reflectarray and the X-Band antenna (ECH). C_2 is the direct coupling between the KaRIn feed and the ECH antenna.

It was important to assess the coupling between KaRIn and the X-band low gain/externally corrugated horn (ECH) antenna to make sure the X-band telecom system did not affect the KaRIn instrument performance. KaRIn operates at 35.75GHz and has a maximum allowed EMI of -113dBm. The KaRIn instrument has two feeds: V- and H-polarized feeds and both couplings were studied for each polarization. The two feeds on the ECH antenna side (i.e. $-Y_{sc}$ side) were considered: H_- and V_{-+} . Hence, the reflectarray radiation patterns considered were H_- and V_{-+} . The contribution from the other side of the spacecraft (H_{++} and V_{++}) are obviously expected to be much lower and therefore were not considered in the analysis.

Each feed and the reflectarray were represented using a SWE. Equation 4 can be applied as the X-band antenna's SWE falls outside the SWE sphere of the reflectarray and feeds.

IV. COUPLING RESULTS

The RF coupling analysis showed that overall there was no major threat to the physical configuration of the nadir deck antennas. The locations of the most antennas was not affected by the results of the coupling analysis except for the X-band low-gain antenna (LGA). All efforts were made to provide very

conservative estimates of output power, antenna gains, receiver sensitivities, and losses.

The location of the X-band LGA was moved from its baseline position within the boundaries of the nadir deck to behind the lip of the AMR reflector in order to shield the AMR horns from excess out-of-band energy. The coupling analysis also showed that as much as 58 dB of the X-band traveling wave tube amplifier's out of band noise required filtering to meet AMR requirements. As a result of these mitigation steps, the risk of the X-band transmitter to nadir deck receivers was deemed low.

KaRIn, while appearing to be a major threat to nadir deck receivers because of its significant output power, is in fact relatively low risk for several reasons. The waveguides used to carry the high power KaRIn RF signals cannot propagate signals lower than 21.1 GHz. KaRIn output power is also significantly attenuated outside of the 35.75 GHz transmit center frequency. Except for the AMR, few receivers are sensitive to Ka-band emissions. The AMR instrument design provided high attenuation at the KaRIn frequencies and will also receive a blanking signal from KaRIn, significantly reducing AMR sensitivity by telling it to "look away" during a KaRIn transmission. The overall source/victim results are shown in Table III.

TABLE III. SWOT VICTIMS AND SOURCES COUPLING RESULTS

| Receiver Victims | Transmitter Sources | | |
|------------------|---|---|--|
| | X-Band | KaRIn Ka-Band | Nadir Altimeter C and Ku Bands |
| KaRIn | Margin: 100 dB at Ka-Band | Not Applicable | Self-compatible with other Ka-band receivers |
| Nadir Altimeter | Margin: >32 dB at C-Band >32 dB at Ku-Band | Margin: Below Ka-Band Waveguide cutoff of 21.1 GHz | Self-compatible with other Ka-band receivers |
| DORIS | Margin: Below X-Band Waveguide Cutoff of 5.26 GHz | Margin: Below Ka-Band Waveguide cutoff of 21.1 GHz | Self-compatible with other Ka-band receivers |
| AMR | Margin: >47 dB at CH1 >55 dB at CH2 >76 dB at CH3 | Margin: CH1: Below Ka-Band Waveguide cutoff of 21.1 GHz 29 dB at CH2 29 dB at CH3 | Margin: C-Band 19 dB at CH1 14 dB at CH2 20 dB at CH2 Ku-Band 23 dB at CH1 18 dB at CH2 24 dB at CH3 |

V. MEASUREMENT AND TEST VALIDATION

Measurements at X-Band and Ka-Band were conducted in order to validate the GRASP analysis models.

A. X-band and Ka-band measurement and validation

An effort was first initiated to define X-band Radiated Susceptibility (RS) levels by two types of analysis—power density calculations and GRASP—and validation of these levels by measurement using an engineering model X-band ECH antenna in an EMC test laboratory. The calculated values that were performed at three nadir deck instrument locations (NA horn, DORIS, AMR horn) correlated with measurements to well within 3 dB in most cases. From calculated levels, a set of recommended RS levels were defined with sufficient margin to encapsulate the worst-case error.

The second set of measurements were performed on a mockup of the Ka-Band feed and reflector boom. Measurements would allow the assessment of the expected electric field levels at the Star Tracker locations. These measurements would allow the comparison and validation of the KaRIn measurements versus the calculated levels at Ka-Band. The mock up included section of the boom, back plate, payload side panel. A Ka-Band source was used with a 200 Watt output power and an ETS-Lindgren HI-6053 three-axes electric field probe measured the fields produced.

B. X-band measurements results versus analysis

The SWOT X-band telecom antenna transmits relatively high power with low gain and thus imposes potentially high Radiated Susceptibility RS03 requirements on other spacecraft RF subsystems. Iterations of the RS requirements from early in the project carried RS03 X-band levels in the range of 50-80 V/m as a consequence of conservative gain estimates (typically -6 dBi to 0 dBi). Modeling and test results of the X-band ECH antenna gain pattern eventually allowed for more refined X-band RS requirement levels, in the range of 10-20 V/m as shown in Table IV. In order to validate the proposed levels and prevent imposing requirements that over/under-test, measurements were carried out to validate existing calculations. The nadir deck-mounted sensitive receiver antennas selected for this exercise were the Nadir Altimeter, DORIS, and AMR.

TABLE IV. SWOT INITIAL RS03 X-BAND REQUIREMENTS BASED ON INITIAL X-BAND ANTENNA GAIN ESTIMATES VERSUS PROPOSED REQUIREMENTS BASED ON CALCULATED ANTENNA GAIN LEVELS

| Radiation Origin | Initial Electric Field RS Specs (V/m) | Proposed Electric Field RS Specs (V/m) | Frequency Band |
|----------------------------------|---------------------------------------|--|---------------------|
| Downlink X-Band Zone 2: NA | 54 | 10 | 8.02 GHz – 8.40 GHz |
| Downlink X-Band Zone 2: DORIS | 52 | 15 | 8.02 GHz – 8.40 GHz |
| Downlink X-Band Zone 2: AMR | 82 | 20 | 8.02 GHz – 8.40 GHz |

Typically, to generate RS03 requirements, the radiated power density equation is used. This makes the tacit assumption that the locations of interest are in the far-field of the transmit antenna. Using the following equation (5):

$$E_{RS03,unmargined} = \sqrt{\frac{P_{tx}G_{tx}(\theta_{victim})}{4\pi R_{victim}^2}}\eta_0 \quad (5)$$

Where:

P_{tx} is the transmitter power [Watts]

$G_{tx}(\theta_{victim})$ is the transmit antenna gain towards the victim unit at an angle

θ_{victim} off of antenna boresight (nadir) [factor, $10^{\frac{dBi}{10}}$]

R_{victim} is the distance to the victim unit [meters]

η_0 is the impedance of free space [ohms]

To verify the applicability of this equation, the Fraunhofer distance—a somewhat-subjective but often-used figure of merit for the far field distance of an electrically large radiator—can be calculated from equation (3). And the additional criteria for the far-field are as follows:

$$\begin{aligned} R &\gg D \\ R &\gg \lambda \end{aligned} \quad (6)$$

In this case, λ is 0.036 m at the transmit frequency of 8.4 GHz. If D is taken to be the aperture of the circular waveguide (24.266 mm), then $R = 0.033$ m. R in this case does not meet the criteria for far field and so D must be modified to include the dimension of the outer-most corrugation (273 mm) (Fig 4).

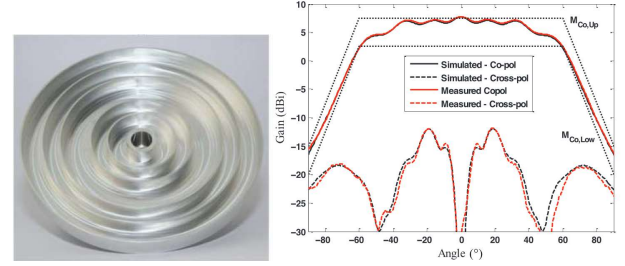


Fig. 4. X-Band externally corrugated horn (ECH) design and antenna gain pattern at 8.4 GHz

Using this value for D , then $R = 4.2$ m. Measurement distances being considered are on the order of 1 meter to 2 meters, so the far field criteria is not strictly met, but neither is the criteria for “electrically-large”: $D/\lambda = 7.6$, which makes the ECH somewhat electrically large but not especially so (typically $D/\lambda > 10$ to be “electrically large”). Gain is also relatively low (about 6 dBi on axis), which makes this criterion more applicable. Given all these ambiguities, it was expected to have some error using the power density equation above, but it is still a useful calculation that should be corroborated by numerical analysis and ultimately by measurement.

Using the SWOT nadir deck layout and X-band antenna gain toward potential victim antennas, the electric field values were calculated using the power density equation (5).

In order to get a higher fidelity result, GRASP simulations were ran to determine the field at these sensitive nadir deck locations. Simulations were run for the antenna in free space and with the spacecraft structure (multipath considered). The results of this simulation are shown in Table V and compared against the measured and far field calculated levels. These

results show relatively good agreement with the far-field power density estimates.

TABLE V. SWOT X-BAND ELECTRIC FIELDS AT RECEIVER LOCATIONS

| Antenna Position | Measured E-Field [V/m] | GRASP MODEL Free Space [V/m] | GRASP MODEL Multi-path [V/m] | Far Field Calculated Field [V/m] |
|------------------|------------------------|------------------------------|------------------------------|----------------------------------|
| NA horn | 4.0 | 3.0 | 3.9 | 4.0 |
| DORIS | 3.4 | 4.5 | 6.3 | 3.3 |
| AMR Horn | 8.4 | 7.0 | 9.8 | 8.1 |

In order to validate the above calculations, measurements were taken with the engineering model X-band ECH antenna. The ECH was placed on the copper bench and the ETS-Lindgren HI-6053 Field Probe was placed at the various sensitive locations at the NA, DORIS and AMR horn locations. A 20dB directional coupler was placed at the output of the 60 Watt power amplifier in order to accurately measure the transmitted power. Using the known transmit power and measured field, the value for field level on the SWOT spacecraft can be determined by scaling the measured value to the appropriate transmit power (60 W) using the power density equation. Multiple measurements were taken at different power levels. All tests were performed at the nominal operating frequency of 8.4 GHz. Set up is in Figures 5 and 6. Table VI summarizes the proposed requirements based on the measurements and analysis of the X-Band electric fields.

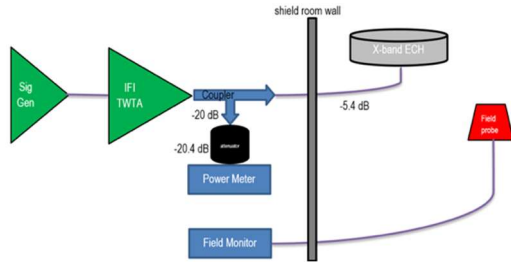


Fig. 5. X-Band measurement set up at 8.4 GHz



Fig. 6. X-Band measurement configuration in EMC chamber lab

TABLE VI. PROPOSED RS REQUIREMENTS FROM MODELS AND MEASUREMENTS

| Radiation Origin | Validated Electric Fields (V/m) | Proposed Electric Fields RS Requirements + Margin (V/m) |
|------------------|---------------------------------|---|
| Zone 2: NA | 4.0 (Measured) | 10 |
| Zone 2: DORIS | 6.3 (GRASP Model) | 15 |
| Zone 2: AMR | 9.8 (GRASP Multi-Path) | 20 |

C. Ka-band measurements results versus analysis

Partial results of a test that measured the electric field as a result of the SWOT KaRIn feed horns at star tracker locations in a mocked-up structure were derived. Configuration and set up are described in Figures 7 and 8. GRASP computer models of the KaRIn radiation pattern predicted that fields in the vicinity of the SWOT star trackers could experience fields ranging from 57 V/m 69 V/m, with a potential maximum of ~200 V/m in some locations a small distance away from proposed star tracker locations. Measurement found correlation to well within 3.8 dB and 0.6 dB in most cases as shown in Table VII.

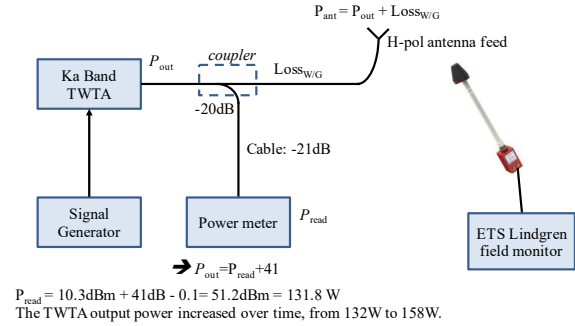


Fig. 7. Ka-Band Measurement Set Up Using TWTA and E-Field Probe

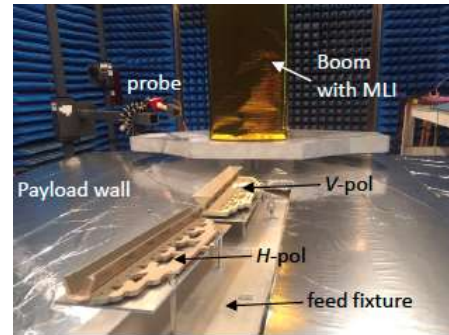


Fig. 8. Ka-Band Measurement Set Up of S/C Panel Mock-up

TABLE VII. SWOT MEASURED KA-BAND LEVELS AT 208.9 WATTS VERSUS CALCULATED, NORMALIZED TO 1413 WATTS

| Measurement Location On Boom | Measured Electric Field (V/m) | TWTA Output Power (Watts) | Measured Field Normalized to 1413 Watts (V/m) | Calculated Field At 1413 Watts (V/m) |
|------------------------------|-------------------------------|---------------------------|---|--------------------------------------|
| Star Tracker 1 | 33.9 | 208.9 | 88.2 | 57.0 |
| Star Tracker 2 | 22.3 | 208.9 | 71.0 | 69.1 |
| Star Tracker 3 | 22.3 | 208.9 | 71.0 | 68.3 |
| Near Boom | 78 | 208.9 | 202.9 | 218.0 |

Based on the validation of the computer model with the actual measurements for the locations of the star trackers, it was recommended that the Ka-band environment derived by modeling be used to establish the RS03 levels, and the star trackers should be subjected to a field larger than 200 V/m (with margin) at Ka-band based on these results.

The Ka-Band radiated susceptibility requirements were assigned by allocating zones on the spacecraft (Figure 9). These were defined for testability purpose at the system level. Based on the validation of the Ka-Band electric field models, it was recommended to use the levels for each of the corresponding zones 1 through 5 with a 6 dB margin added. Figure 10 shows the corresponding Ka-Band RS requirement for each corresponding zone location. Table VIII shows the comparison of the initial RS requirements based on first order coupling analysis and the more refined GRASP coupling models.

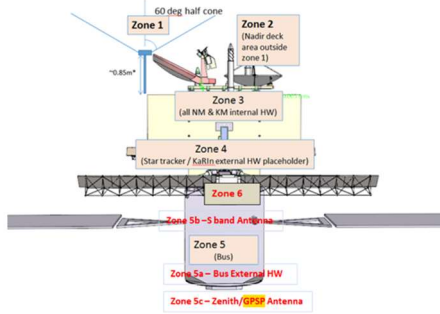


Fig. 9. Radiated susceptibility electric field limit zone definitions

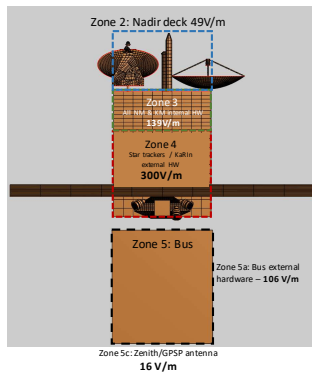


Fig. 10. Zone radiated susceptibility requirements for Ka-band based on model

TABLE VIII. SWOT INITIAL KARIN KA-BAND 35.5 GHz TO 36 GHz RS LEVELS VERSUS PROPOSED KARIN RS LEVELS BASED ON MODELS

| Zone Location On SWOT | Electric Field (V/m) RS Requirement Levels At Prelim Design Review | Electric Field (V/m) RS Requirement Levels At Critical Design Review |
|--|--|--|
| Zone 2 (Nadir Instruments) | 244 | 49 |
| Zone 3 (Nadir Module) | 73 | 139 |
| External Units In Zone 5a (spacecraft bus) | 298 | 106 |
| Zone 5c (spacecraft bus) | TBD | 16 |

Error between measurement and all forms of calculation fell well within the 6 dB margin added to typical field calculations, although the smallest error across a wide variety of situations can be found from numerical calculations done in GRASP, especially in the free-space calculation. The multipath calculation is especially accurate for the NA horn but exhibits slightly more error at the DORIS and AMR horn locations. This can be attributed to the relatively large differences in the multipath environment of the spacecraft simulation compared to the

EMC chamber, which did not have absorber in all possible places around the antenna or probe. It is also worth noting that the hand calculations agree very well with measurement, providing additional confidence where a far-field assumption is reasonable. As a result, it is recommended that values derived from analysis, especially those from GRASP numerical analysis, be used as the starting point for defining RS03 levels.

CONCLUSION

In defining RS requirements for a spacecraft with multiple number of receivers and transmitters in close proximity to each other, it is highly recommended that an RF coupling analysis be initially performed in order to determine if the mechanical configuration of the receiver and transmitter antennas presents a risk to the functionality and safety of sensitive receiver instruments. From the results of the coupling analysis, radiated susceptibility requirements can be derived to better reflect actual levels with adequate test margin. It is recommended that the requirements also be validated with actual measurements using mock-up antenna configurations in order to avoid imposing overly conservative RS requirements and, hence, avoid over-testing sensitive instruments.

ACKNOWLEDGMENTS

The research described in this paper was performed at the Jet Propulsion Laboratory, California Institute of Technology, for the National Aeronautics and Space Administration.

COPYRIGHT

Copyright 2018 California Institute of Technology. U.S. Government sponsorship acknowledged.

REFERENCES

- [1] N. Chahat, L. Amaro, J. Harrell, C. Wang, P. Estabrook, and B. Stan, "X-band choke horn telecom antenna for interference mitigation on NASA's SWOT mission," *IEEE Trans. on Antennas Propagation*, vol. 64, no. 6, pp. 2075-2082, June 2016.
- [2] H. W. Ott, *Electromagnetic Compatibility Engineering*. Hoboken, NJ, USA: Wiley, 2009.
- [3] J. D. Kaus, "Antennas" 2nd Ed., McGraw-Hill, 1988.
- [4] <http://www.ticra.com/products/software/grasp>
- [5] L. Salghetti Drioli, L. J. Foged, F. Saccardi, L. Scialacqua, "Analysis of spacecraft antenna farm interaction with equivalent current technique," *2015 9th European Conference on Antennas and Propagation (EuCAP)*.
- [6] Kun-A Lee, Jae-ho Rhee, Young-Mann Cho, Ji-Eun Baek, Kwang-Cheol Ko, "Damage prediction of RF system affected by electromagnetic pulse," *2013 19th IEEE Pulsed Power Conference*.
- [7] N. Chahat, R. Hodges, "Ka-band radar interferometer (KaRIn) Coupling Summary: updated results with REFANA v2.0," Presentation, Jet Propulsion Laboratory, Pasadena, CA, USA, May 2016.
- [8] E. Gonzales, "SWOT Nadir Deck RF Coupling Analysis Results," Jet Propulsion Laboratory, Pasadena, CA, USA, IOM 5137-15-055A, May 2016.
- [9] N. Chahat, P. Estabrook, S. Butman, C. Wang, "Coupling Assessment Between the X-band Telecom Antenna and SWOT's Instruments and DSN," Jet Propulsion Laboratory, Pasadena, CA, USA, 337-NC PE SB CW-20150708-175, Sept. 2015.
- [10] E. Gonzales, "SWOT KaRIn EMC RS03 Verification by Measurement at Star Tracker Locations," Jet Propulsion Laboratory, Pasadena, CA, USA, IOM 5137-16-107, Nov. 2016.
- [11] D. Russel, "AMR-S RFI Susceptibility," Jet Propulsion Laboratory, Pasadena, CA, USA, IOM SWOT-8550-16-002, March 2016.

